A New Cyanofluorene–Triphenylamine Copolymer: Synthesis and Photoinduced Intramolecular Electron Transfer Processes

7 AUTHORS, INCLUDING:

Mohamed E El-Khouly
Kafrelsheikh University
129 PUBLICATIONS **3,162** CITATIONS

SEE PROFILE

yu Chen
East China University of Science and Techn…
105 PUBLICATIONS **2,236** CITATIONS

SEE PROFILE

Mustafa Supur
University of Alberta
20 PUBLICATIONS **226** CITATIONS

SEE PROFILE

A New Cyanofluorene–Triphenylamine Copolymer: Synthesis and Photoinduced Intramolecular Electron Transfer Processes

Ying Lin,[a] Mohamed E. El-Khouly,*[b] Yu Chen,*[a] Mustafa Supur,[b] Lingling Gu,[a] Yongxi Li,[a] and Shunichi Fukuzumi*[b]

Abstract: A new π-conjugated copolymer, namely, poly{cyanofluore-*alt*-[5-(*N,N*′-diphenylamino)phenylenevinylene]} ((CNF–TPA)$_n$), was synthesized by condensation polymerization of 2,2′-(9,9-dioctyl-9H-fluorene-2,7-diyl)diacetonitrile and 5-(*N,N*′-diphenylamino)-benzene-1,3-dicarbaldehyde by using the Knoevenagel reaction. By design, diphenylamine, alkylfluorene and poly(*p*-phenylenevinylene) linkages were combined to form a (CNF–TPA)$_n$ copolymer which exhibits high thermal stability and glass-transition temperature. Photodynamic measurements in polar benzonitrile indicate fast and efficient photoinduced electron transfer

Keywords: copolymerization · electron transfer · knoevenagel reaction · polyfluorene · polymerization

($\approx 10^{11}$ s^{-1}) from triphenylamine (TPA) to cyanofluorene (CNF) to produce the long-lived charge-separated state (90 μs). The finding that the charge-recombination process of (CNF$^{\cdot-}$–TPA$^{\cdot+}$)$_n$ is much slower than the charge separation in polar benzonitrile suggests a potential application in molecular-level electronic and optoelectronic devices.

Introduction

Since the first conducting polymer was discovered by Shirakava in 1977,[1] a wide range of polymers, such as poly(*p*-phenylenevinylene) (PPV), polythiophene (PT), poly(*p*-phenylene) (PPP), polyfluorene (PF), and their derivatives, have been extensively investigated for use in polymeric light-emitting diodes (PLEDs).[2–4] Among the identified light-emitting polymers, polyfluorenes (PFs) have emerged as one of the most promising materials owing to their high photoluminescence quantum yields, good charge-transport properties, better thermal and chemical stability, and facile functionalization at the C9 position of the fluorene unit,

which may offer an opportunity to reduce interchain interactions and thereby improve the optoelectronic properties of the resulting polymers.[5–8] Essentially, electron injection is more difficult than hole injection for conjugated polymer-based PLEDs. A good way to address this problem is to increase the electron affinity of polymer to reduce the electron injection barrier.[9] The electron-withdrawing cyano (CN) group has been used to improve the electron-transport properties of the material[10,11] because it can not only adjust the electron mobilities but also alter the electron affinity of the material, thus facilitating electron injection.[10]

On the other hand, triphenylamine (TPA)-based hole-transporting materials have been widely used in organic and polymeric LEDs due to their low ionization potentials, tridimensional steric profile, and good UV light harvesting properties.[12] The biggest disadvantages of TPA lie in its crystallization, surface diffusion, relatively low thermal stability, and also in the difficulties of fabricating devices. These drawbacks that restrict its applications in LEDs can be overcome by incorporating TPA into the polymer backbone.

Herein, we designed a new π-conjugated functional polymer, poly{cyanofluore-*alt*-[5-(*N,N*′-diphenylamino)phenylenevinylene]} ((CNF–TPA)$_n$; CNF=cyanofluorene), in which TPA, alkylfluorene, and PPV (poly(*p*-phenylene vinylene)) linkages were combined to form a new polymer with CN functional groups. We also studied the optical properties and photoinduced electron transfer processes of the new po-

[a] Y. Lin, Prof. Dr. Y. Chen, L. Gu, Y. Li
Key Laboratory For Advanced Materials
Department of Chemistry
East China University of Science and Technology
130 Meilong Road, Shanghai 200237 (China)
E-mail: chentangyu@yahoo.com

[b] Dr. M. E. El-Khouly, M. Supur, Prof. Dr. S. Fukuzumi
Department of Material and Life Science
Graduate School of Engineering, Osaka University
SORST (Japan) Science and Technology Agency (JST)
Suita, Osaka 565-0871 (Japan)
E-mail: fukuzumi@chem.eng.osaka-u.ac.jp

lymer. A 9,9-dioctyl-9*H*-fluorene moiety was chosen as part of the resulting polymer backbone due to its known high photo- and electro-luminescence efficiencies, good film-forming properties, high solubility, and thermal stability. This polymer was synthesized by condensation polymerization of 2,2′-(9,9-dioctyl-9*H*-fluorene-2,7-diyl)diacetonitrile[9a,13] (**1**) and 5-(*N*,*N*-diphenylamino)benzene-1,3-dicarbaldehyde[14] (**2**) by using the Knoevenagel reaction (see Scheme 1). The resulting (CNF–TPA)$_n$ copolymer, which is highly soluble in many common organic solvents, exhibits fast charge-separation and slow charge-recombination processes in polar benzonitrile.
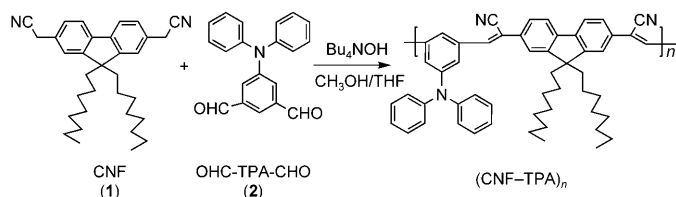
Scheme 1. Synthesis of (CNF–TPA)$_n$ copolymer.

Results and Discussion

Yoon et al.[11d] reported a similar copolymer, namely, poly[2-(7-{1-cyano-2-[4-(phenyl-*p*-tolyl-aminophenyl)vinyl]-9,9-di-hexyl-9H-fluoren-2-yl}but-2-enenitrile)] (TFCN–PPV), in which the electron-withdrawing CN group was incorporated into the polymer backbone. From Figure 1, it can clearly be seen that the main chain of TFCN–PPV is apparently twisted compared with that of (CNF–TPA)$_n$. Distortion of the conjugation and coplanarity of the polymer backbone and an increase of the interchain distance in the TFCN–PPV system would hinder both intra- and interchain charge-transfer processes and possibly lead to lower device performance.
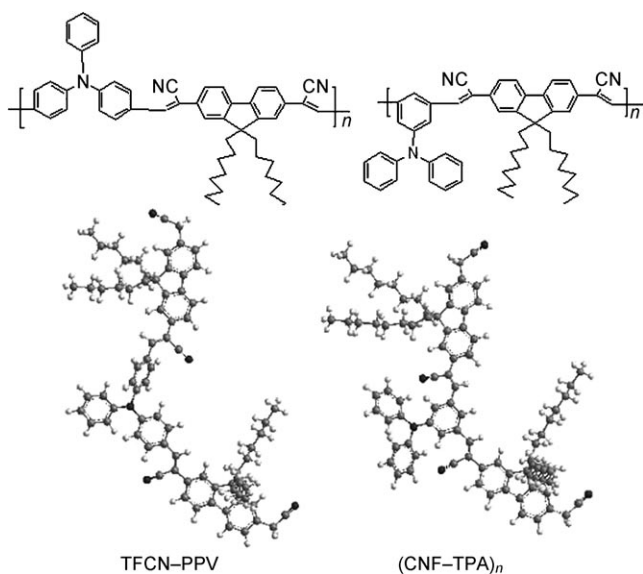

Figure 1. Optimized structures of TFCN–PPV and (CNF–TPA)$_n$.

Comparably, (CNF–TPA)$_n$, which has the diphenylamine group as a side chain, would be expected to be more favorable for charge transfer as a result of the noninterrupted conjugated main chains, resulting in a possible improvement in the corresponding device efficiency.

The ^{1}H NMR spectroscopy results of (CNF–TPA)$_n$ in CDCl$_3$ shows that the aromatic and olefin proton signals appear at $\delta = 6.9$–8.0 ppm, whereas the proton signals of the alkyl groups in the alkylfluorene unit are located around $\delta = 0.5$–2.1 ppm. A sharp absorption band appeared at $\tilde{v} = 2220$ cm^{-1} in the FT-IR spectrum can be logically assigned to the CN stretching vibration mode in the vinylene linkages.[11d] As expected, (CNF–TPA)$_n$ displays a high single glass transition temperature ($T_g = 136$ °C, Figure 2) that is
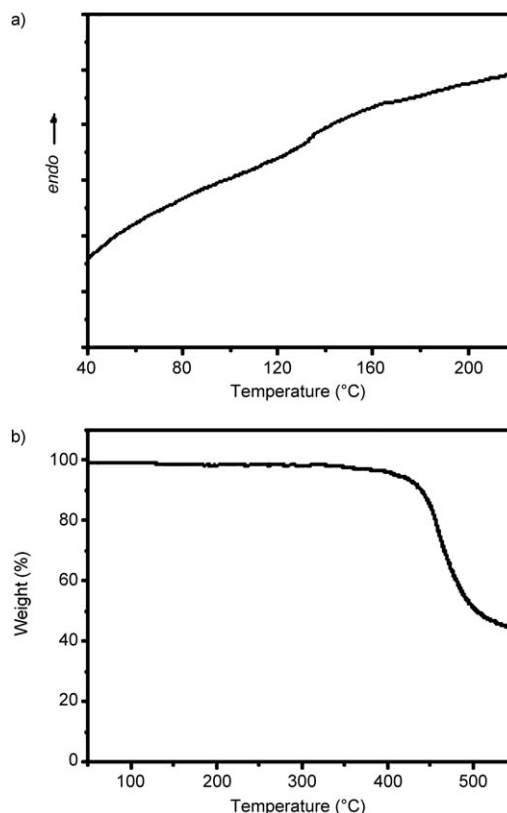

Figure 2. a) DSC trace and b) TGA thermogram of (CNF–TPA)$_n$ measured under nitrogen.

much higher than those of poly(9,9-dioctylfluorene) (≈ 51 °C)[15] and poly(9,9-dihexylfluorene) (≈ 55 °C)[16] due to the incorporation of TPA moieties onto the polymer backbone. The decomposition temperature (10% weight loss) of (CNF–TPA)$_n$ is 440 °C, higher than that of TFCN–PPV (≈ 383 °C) reported by Yoon et al.[11d] This finding suggests that (CNF–TPA)$_n$ has much better thermal stability than TFCN–PPV. It is worth mentioning that better thermostability of component materials is critical for the lifetime of solar cells.[17]

The main absorption peaks of **1** are located at $\lambda = 266$, 297, and 309 nm, whereas the spectrum for **2** shows four ab-

sorption peaks at $\lambda = 270, 296, 343,$ and 419 nm (see the Supporting Information, Figure S1). After copolymerization, (CNF–TPA)$_n$ shows two stronger absorption peaks at $\lambda = 290$ and 385 nm. These peaks are associated with the π–π* transition of the entire molecular backbone for (CNF–TPA)$_n$.[18] The absorption bands (Figure S2 in the Supporting Information) in polar THF, benzonitrile (PhCN), and dimethylformamide (DMF) exhibited a 5 nm redshift compared with that in toluene, which suggests a small dipole moment interaction. Figure 3 compares the changes of the UV/Vis
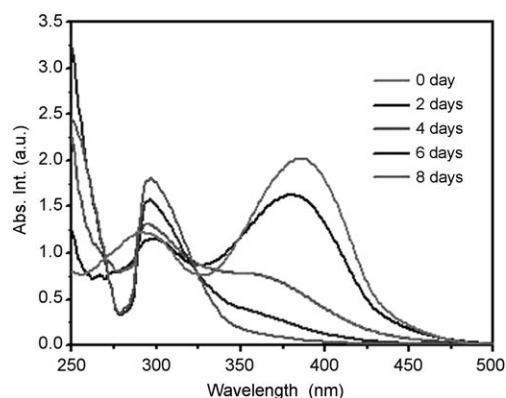

Figure 3. The changes in the UV/Vis absorption spectra of (CNF–TPA)$_n$ in THF before and after exposure to ambient light.

absorption spectra of a dilute solution of the polymer in THF before and after exposure to ambient light. Before exposure, the color of the solution was light yellow. The intensity of the peak at $\lambda = 385$ nm decreased gradually with increased exposure to daylight and was simultaneously followed by an increase in the absorption intensity at $\lambda = 290$ nm. At 8 d, the color of the THF solution gradually turned from light yellow to colorless. A possible explanation for this observation is that the TPA moieties in the polymer structure are not as stable as expected and the visible light accelerates their photodissociation. When molecules containing Group V elements with triphenyl substituents, such as Ph_3N, Ph_3P, Ph_3As, Ph_3Sb, and/or Ph_3Bi, are irradiated with ultraviolet light, photodissociation occurs and the maximum absorption band becomes weaker and broader.[19,20] Furthermore, the UV/Vis absorption bands of a thin film of (CNF–TPA)$_n$ are apparently broader, but the position of the absorption peaks remain almost unchanged compared with a dilute solution in solvents such as anhydrous THF and toluene. This result suggests that the aggregation of (CNF–TPA)$_n$ in solution, even in the solid state, is almost negligible. The aggregates are usually depicted as a coplanar association of the aromatic rings in the polymer and are driven by enhanced Van der Waals attractive forces between the aromatic rings. The tendency to aggregate is mainly dependent on the structural characteristics of the conjugated polymer and is usually unfavorable for the fluorescence efficiency and emission color of the material.

Given that the studied copolymers contain donor and acceptor units, we started to study the photoinduced intramolecular events by measuring the steady-state fluorescence spectra with $\lambda = 380$ nm excitation light (which selectively excites the CNF entity). As shown in Figure 4, the emission
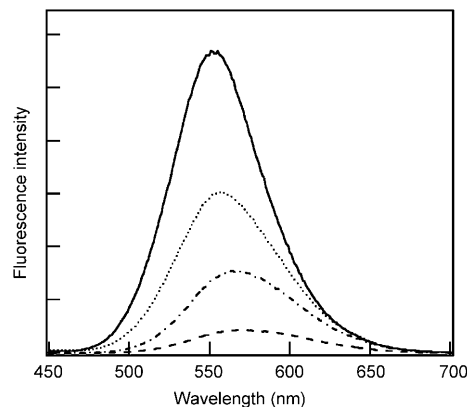

Figure 4. Steady-state fluorescence spectra of (CNF–TPA)$_n$ in toluene (——), THF (·····), PhCN (–·–·), and DMF (-----); $\lambda_{ex} = 380$ nm.

spectrum of the CNF moiety in toluene shows a green emission band at $\lambda = 552$ nm, from which the energy of the singlet state was estimated as 2.24 eV. As the polarity of the solvent increased, the emission band of the CNF moiety was observed to get broader and become redshifted ($\lambda = 555$ (THF), 564 (PhCN), and 568 nm (DMF)). The finding that the fluorescence intensity decreased as the solvent polarity increased suggests that the quenching process is probably due to the electron-transfer process from TPA to ^1CNF*.

The electron-transfer process was supported by the thermodynamics of the electron-transfer processes. The electrochemical measurements were carried out by using cyclic voltammetry (CV) and differential pulse voltammetry (DPV) at a glassy carbon electrode in deaerated benzonitrile with 0.1 M tetrabutylammonium hexafluorophosphate (TBAPF$_6$) at room temperature (Figure 5). The potentials were measured against Ag/AgNO$_3$ as the reference electrode. All potentials (vs. Ag/Ag$^+$) were converted to values versus SCE by adding 0.29 V.[21] Both techniques show the first oxidation potential (E_{ox}) of the TPA entity at 0.67 V versus Ag/Ag$^+$, which corresponds to 0.96 V versus SCE, whereas the first reduction potential (E_{red}) of the CNF entity was found to be -1.44 V versus Ag/Ag$^+$, which corresponds to -1.15 V versus SCE. Based on the first oxidation potential of the TPA, the first reduction potential of CNF, and the energy of the excited singlet state of CNF (2.24 eV), the driving forces for the charge-recombination process ($-\Delta G_{CR}$) and the intramolecular charge separation ($-\Delta G_{CS}$) were calculated to be 2.06 and 0.18 eV, respectively. The negative ΔG_{CS} values in polar solvents suggest an exothermic charge-separation process occurs to form the radical ion pair (CNF$^{\cdot-}$–TPA$^{\cdot+}$)$_n$.

To gain insights into the geometry and electronic structures of (CNF–TPA)$_n$, computational studies were per-
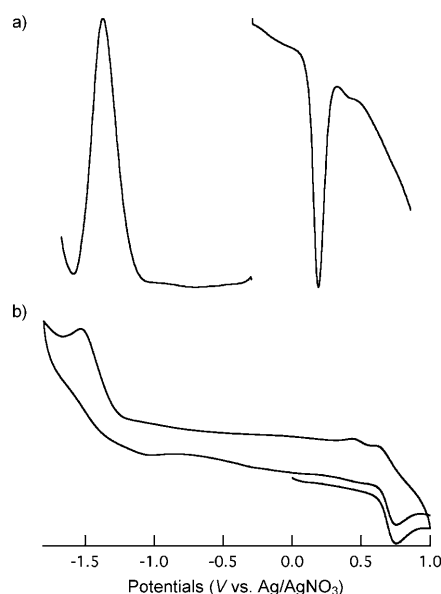
Figure 5. a) Differential pulse voltammogram and b) cyclic voltammogram of $(CNF–TPA)_n$ in deaerated benzonitrile with $TBAPF_6$ (0.1 M) as the supporting electrolyte; sweep rate 50 mVs⁻¹.

formed by using DFT at the B3LYP/6-31G level (Figure 6). The accuracy of these methods for the electron affinities of aromatic compounds has been demonstrated by Schaefer and co-workers.[22] From the optimized structures, the majority of the electron distribution of the highest occupied molecular orbital (HOMO) was found to be located on the TPA entity. The electron distribution of HOMO−1 and HOMO−2 were found to be over the neighboring TPA units, which indicates that the hole migration occurs between the TPA entities. On the other hand, the electron distributions of the lowest unoccupied molecular orbitals (LUMOs) were found to be mutually located over the CNF entities. The distinct distribution of HOMO and LUMO
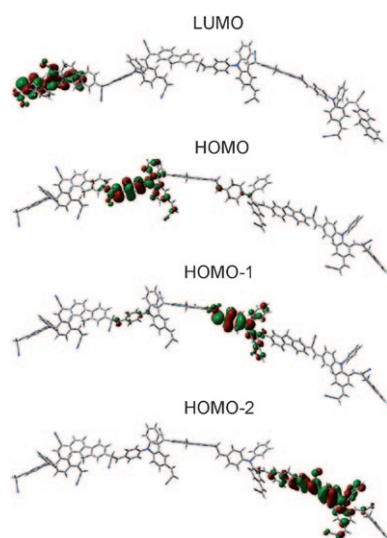

Figure 6. Frontier HOMOs and LUMO of $(CNF–TPA)_n$ calculated by ab initio B3LYP/6-31G methods.

levels in $(CNF–TPA)_n$ suggests that the electron transfer goes from TPA to CNF to form $(CNF^{•–}–TPA^{•+})_n$.

Experimental proof and kinetic characterization of the electron-transfer process from singlet state of CNF to TPA of $(CNF–TPA)_n$ can be obtained by femtosecond transient measurements in deaerated benzonitrile and toluene by using $\lambda = 390$ nm laser light (Figure 7 and Figure S3 in the
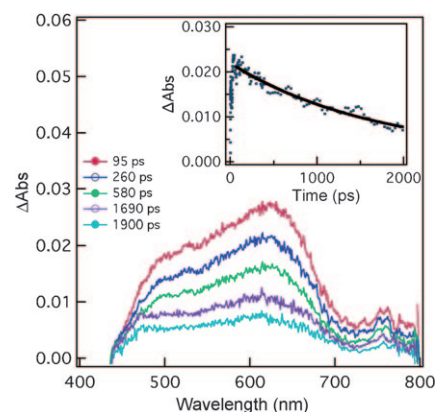

Figure 7. Femtosecond transient spectra of $(CNF–TPA)_n$ in deaerated benzonitrile obtained by using $\lambda = 390$ nm laser light. Inset: Time profile of $TPA^{•+}$ at $\lambda = 640$ nm.

Supporting Information). The spectra in toluene and benzonitrile show the formation of the radical ion pair $(CNF^{•–}–TPA^{•+})_n$ by observing the maximum absorption bands in the visible region with maxima at $\lambda = 640$ nm, which have been assigned to the TPA radical cation $(TPA^{•+})$. The absorption of $TPA^{•+}$ in the visible region was confirmed by mixing the $(CNF–TPA)_n$ with the one-electron oxidant $[Ru(bpy)_3]^{3+}$ (Figure S4 in the Supporting Information). It is worth mentioning here that broad absorption bands with maxima at $\lambda = 500$ and 750 nm may arise from the overlapping of the radical species of $TPA^{•+}$ and the CNF radical anion $(CNF^{•–})$.[23] The time profile of $TPA^{•+}$ at $\lambda = 640$ nm was employed to determine the rates of the charge-separation (k_{CS}) and charge-recombination (k_{CR}) processes. As shown in Figure 7, inset, the time profile of $TPA^{•+}$ shows a rapid rise in the first 40 ps followed by slow decay. From the initial rise, we determined the rates of the charge-separation process in toluene and benzonitrile to be 8.3×10^{10} and 1.1×10^{11} s⁻¹, respectively. From the decay of $TPA^{•+}$ in toluene, the rate of the charge-recombination (k_{CR}) was calculated to be 1.1×10^{10} s⁻¹, from which the lifetime of the charge-separated state (τ_{CS}) was determined as 94 ps. In benzonitrile, however, the k_{CR} value (6.2×10^8 s⁻¹) was found to be significantly lower compared with that in toluene. Based on the k_{CR} value, the τ_{CS} value was determined as 1.6 ns.

Because the decay profile is not completely decayed on the picosecond time scale, we performed nanosecond measurements to follow the slow decay of $TPA^{•+}$. The nanosecond transient absorption spectra in deaerated benzonitrile with $\lambda = 355$ nm laser light (Figure 8) exhibited absorption bands of both $CNF^{•–}$ and $TPA^{•+}$, similar to those observed
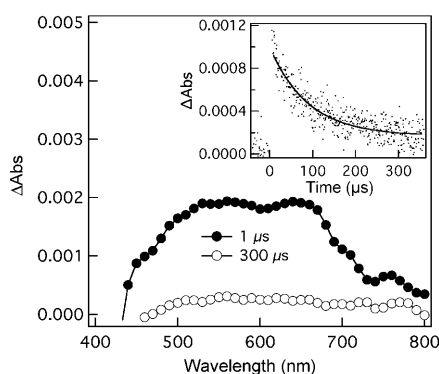
Figure 8. Nanosecond transient absorption spectra of $(CNF–TPA)_n$ in deaerated benzonitrile obtained by using $\lambda = 355$ nm laser light. Inset: Time profile of $TPA^{\cdot +}$ at $\lambda = 640$ nm.

in Figure 7. An important finding is that the $CNF^{\cdot -}$ and $TPA^{\cdot +}$ recombined slowly with a rate constant of $1.1 \times 10^4 \, s^{-1}$, from which the lifetime of the radical ion pair $(CNF^{\cdot -}–TPA^{\cdot +})_n$ was found be long-lived (90 μs) with a quantum yield of 15%.[24,25] This long lifetime of $(CNF^{\cdot -}–TPA^{\cdot +})_n$ can be explained by the hole migration between $TPA^{\cdot +}$ groups and the electron shift between $CNF^{\cdot -}$ groups along the polymer chain (Scheme 2).
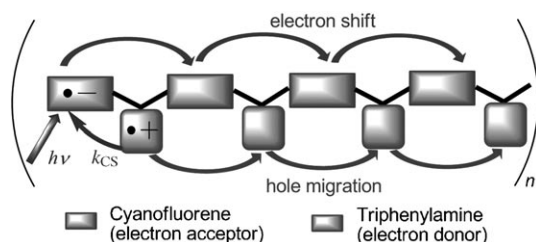
Scheme 2. Photoinduced charge separation from TPA to CNF followed by hole migration and electron shift along the polymer chain.

Conclusions

A new π-conjugated copolymer, $(CNF–TPA)_n$, was synthesized by condensation polymerization of 2,2′-(9,9-dioctyl-9H-fluorene-2,7-diyl)diacetonitrile and 5-(N,N-diphenylamino)benzene-1,3-dicarbaldehyde by using the Knoevenagel reaction. $(CNF–TPA)_n$ exhibited a high glass transition temperature and thermal stability up to 440 °C. This soluble polymer exhibited fast charge separation of about $10^{11} \, s^{-1}$ in polar and nonpolar solvents. The rate of charge recombination in polar benzonitrile was recorded to be $6.2 \times 10^8 \, s^{-1}$ from the femtosecond measurements, whereas in the nanosecond measurements it was found to be $1.1 \times 10^4 \, s^{-1}$. The existence of multiple CR processes of $(CNF–TPA)_n$ may be related to the distance between the radical species, taking in consideration the hole migration between the TPA entities and the electron shift between the CNF entities. This long-lived radical ion pair, $(CNF^{\cdot -}–TPA^{\cdot +})_n$, may be useful in improving the photovoltaic response in terms of the photocurrent and photovoltage generation.

Experimental Section

General: The syntheses prior to the termination reaction were carried out under purified argon. Tetra-n-butylammonium hydroxide (Bu₄NOH, 40% in methanol) was purchased from ABCR. All other chemicals were purchased from Aldrich and used without further purification. Organic solvents were purified, dried, and distilled under dry nitrogen. IR spectra were recorded by using a Nicolet Nagma-IR 550 spectrophotometer using KBr pellets. The UV/Vis spectral measurements were carried out by using a Shimadzu UV-2450 spectrophotometer. The thermal properties of the samples were measured by using a Perkin–Elmer Pyris 1 thermogravimetric analyzer in under an N_2 flow (100 mL min^{-1}). Steady-state fluorescence spectra were measured by using a Shimadzu RF-5300 PC spectrofluorophotometer equipped with a photomultiplier tube with high sensitivity in the $\lambda = 700$–800 nm region. Samples for fluorescence measurement were dissolved in dry toluene or benzonitrile, filtered, transferred to a long quartz cell, and then capped and bubbled with high-purity argon (without O_2 and moisture) for at least 15 min before measurement.

Cyclic voltammetry was performed at 298 K by using an ALS630B electrochemical analyzer in deaerated benzonitrile that contained recrystallized tetra-n-butylammoniumhexafluorophosphate (TBAPF₆; 0.1 M) as the supporting electrolyte. A conventional three-electrode cell was used with a platinum working electrode (surface area of 0.3 mm²) and a platinum wire as the counter electrode. The Pt working electrode (BAS) was routinely polished with BAS polishing alumina suspension and rinsed with acetone before use. The measured potentials were recorded with respect to an Ag/AgNO₃ (0.01 M) reference electrode. All electrochemical measurements were carried out under argon (atmospheric pressure).

Femtosecond transient absorption spectroscopy experiments were conducted by using an ultrafast source (Integra-C (Quantronix)), an optical parametric amplifier (TOPAS (Light Conversion)), and a commercially available optical detection system (Helios (Ultrafast Systems)) The source for the pump and probe pulses were derived from the fundamental output of Integra-C ($\lambda = 780$ nm, 2 mJ pulse^{-1}, full width at half maximum (fwhm) 130 fs) at a repetition rate of 1 kHz. 75% of the fundamental output of the laser was introduced into TOPAS, which has optical frequency mixers that result in a tunable range of $\lambda = 285$–1660 nm. The rest of the output was used for white light generation. Typically, 2500 excitation pulses were averaged for 5 s to obtain the transient spectrum at a set delay time. Kinetic traces at appropriate wavelengths were assembled from the time-resolved spectral data. All measurements were conducted at 298 K. The transient spectra were recorded by using fresh solutions for each laser excitation.

The nanosecond transient absorption measurements were measured by using a Panther OPO pumped by Nd:YAG laser (Continuum, SLII-10, fwhm 4–6 ns) at $\lambda = 355$ nm with the powers of 1.5 and 3.0 mJ pulse^{-1}. The transient absorption measurements were performed by using a continuous xenon lamp (150 W) and an InGaAs-PIN photodiode (Hamamatsu 2949) as the probe light and detector, respectively. The output from the photodiodes and a photomultiplier tube was recorded by using a digitizing oscilloscope (Tektronix, TDS3032, 300 MHz).

DFT calculations were performed by using a COMPAQ DS20E computer. Geometry optimizations were carried out by using the B3LYP functional and 6-31G basis set, with the unrestricted Hartree–Fock (UHF) formalism and as implemented in the Gaussian 03 program.[26] Graphical outputs of the computational results were generated with GaussView (v. 3.09, developed by Semichem).

Synthesis of $(CNF–TPA)_n$: 2,2′-(9,9-dioctyl-9H-fluorene-2,7-diyl)diacetonitrile (**1**, 227 mg, 0.484 mmol) and 5-(N,N-diphenylamino)benzene-1,3-dicarbaldehyde (**2**, 146 mg, 0.484 mmol) were added to a mixture of anhydrous THF (25 mL) and freshly distilled methanol (12 mL) and heated to 65 °C under highly purified nitrogen, then Bu₄NOH (0.30 mL) in meth-

anol (1 M) was added. After heating at reflux for 12 h, the reaction mixture was slowly cooled to 0 °C and then treated with methanol (30 mL). The obtained crude product was collected, redissolved in anhydrous THF, and then reprecipitated from methanol to give an organic solid powder that was dried under vacuum and further purified by Soxhlet extraction with methanol for 72 h to give (CNF–TPA)$_n$ (154 mg). ^{1}H NMR (500 MHz, CDCl$_3$): $\delta = 0.52$–0.61 (br s, 4H), 0.76–0.81 (br s, 6H), 1.04–1.18 (br s, 20H), 1.92–1.96 (br s, 4H), 2.03–2.10 (br s, 4H), 6.92 (br s, 1H), 7.12–7.22 (br s, 7H), 7.31–7.41 (br s, 4H), 7.57–7.60 (br s, 5H), 7.66–7.76 (br s, 3H), 7.94 ppm (br s, 1H); SEC/GPC: $M_w = 4.1 \times 10^4$, $M_n = 1.5 \times 10^4$, $M_w/M_n = 2.81$.

[1] H. Shirakawa, E. J. Louis, A. G. MacDiarmid, C. K. Chiang, A. J. Heeger, *Chem. Commun.* **1977**, 578–580.

[2] A SCIFinder 2007 search gave 534 hits for the last seven years for references dealing with PLEDs (SCIFinder Scholar, ACS, Washington, **2007**).

[3] a) S. Miyata, H. S. Nalwa, *Organic Elecroluminescent Materials and Devices*, Gordon and Breach Publishers, Amsterdam, **1997**; b) C. J. Neef, J. P. Ferrais, *Macromolecules* **2000**, *33*, 2311–2314; c) Y. M. Huang, W. Ge, J. W. Y. Lam, T. B. Zhang, *Appl. Phys. Lett.* **1999**, *75*, 4094–4096; d) G. Grem, V. Martin, F. Meghdadi, C. Paer, J. Stampfl, J. Sturm, S. Tasch, G. Leising, *Synth. Met.* **1995**, *71*, 2193–2194; e) H. Nishino, G. Yu, A. J. Heeger, T. A. Chen, R. D. Rieke, *Synth. Met.* **1995**, *68*, 243–247; f) A. D. Schlütter, *J. Polym. Sci. Part A* **2001**, *39*, 1533–1556; g) Z. Zheng, K.-H. Yim, M. S. M. Saifullah, M. E. Welland, R. H. Friend, J.-S. Kim, W. T. S. Huck, *Nano. Lett.* **2007**, *7*, 987–992; h) M. Leclerc, *J. Polym. Sci. Part A* **2001**, *39*, 2867–2873; i) J. H. Burroughes, D. D. C. Bradley, A. R. Brown, R. N. Marks, K. Mackay, R. H. Friend, *Nature* **1990**, *347*, 539–541; j) H. J. Su, F. L. Wu, C. F. Shu, Y. L. Tung, Y. Chi, G. H. Lee, *J. Polym. Sci. Part A* **2005**, *43*, 859–869; k) Y. Jin, J. Jee, K. Kim, J. Kim, S. Song, S. H. Park, K. Lee, H. Suh, *Polymer* **2007**, *48*, 1541–1549.

[4] A. Kraft, A. C. Grimsdale, A. B. Holmes, *Angew. Chem.* **1998**, *110*, 416–443; *Angew. Chem. Int. Ed.* **1998**, *37*, 402–428.

[5] a) Y. Chen, Y. Araki, J. Doyle, A. Strevens, O. Ito, W. J. Blau, *Chem. Mater.* **2005**, *17*, 1661–1666; b) Y. Chen, Y. Lin, M. E. El-Khouly, N. He, A. Yan, Y. Liu, L. Z. Cai, O. Ito, *J. Polym. Sci. Part A* **2008**, *46*, 4249–4253.

[6] a) M. J. Winokur, M. Cheun, M. Knaapila, A. P. Monkman, U. Scherf, *Phys. Rev. B* **2007**, *75*, 113202/1–113202/4; b) A. Hayer, A. L. T. Khan, R. H. Friend, A. Kohler, *Phys. Rev. B* **2005**, *71*, 241302/1–241302/4; c) S. Doi, T. Yamada, Y. Tsubata, M. Ueda, *Proc. SPIE* **2004**, *5519*, 161; d) B. D. Chin, L. Duan, M.-H. Kim, S. T. Lee, H. K. Chung, *Appl. Phys. Lett.* **2004**, *85*, 4496–4498; e) L. Ding, F. E. Karasz, Y. Lin, Y. Pang, L. Liao, *Macromolecules* **2003**, *36*, 7301–7307; f) F. L. Wu, R. Dodda, D. S. Reddy, C. F. Shu, *J. Mater. Chem.* **2002**, *12*, 2893–2897; g) T. M. Brown, R. H. Friend, I. S. Millard, D. J. Lacey, J. H. Burroughes, F. Cacialli, *Appl. Phys. Lett.* **2001**, *79*, 174–176.

[7] a) W. Z. Wang, G. Z. Yang, T. X. Liu, J. Yu, Y. Jiang, *J. Polym. Sci. Part A* **2008**, *46*, 790–802; b) Y. Fu, M. Sun, Y. Wu, Z. Bo, D. Ma, *J. Polym. Sci. Part A* **2008**, *46*, 1349–1356; c) Q. Peng, L. Yan, D. Chen, F. Wang, P. Wang, D. Zou, *J. Polym. Sci. Part A* **2007**, *45*, 5296–5307; d) E. Wang, C. Li, J. Peng, Y. Cao, *J. Polym. Sci. Part A* **2007**, *45*, 4941–4949; e) G. Nie, X. Han, S. Zhang, Q. Wei, *J. Polym. Sci. Part A* **2007**, *45*, 3929; f) M. C. Yuan, P. I. Shih, C. H. Chien, C. F. Shu, *J. Polym. Sci. Part A* **2007**, *45*, 2925–2937; g) C. H. Chien, P. I. Shih, F. I. Wu, C. F. Shu, Y. Chi, *J. Polym. Sci. Part A* **2007**, *45*, 2073–2084; h) Y. H. Kim, S. Y. Jung, S. O. Jung, M. H. Park, S. K. Kwon, *J. Polym. Sci. Part A* **2006**, *44*, 4923–4931.

[8] a) W. Niu, M. D. Smith, J. J. Lavigne, *J. Am. Chem. Soc.* **2006**, *128*, 16466–16467; b) F. Huang, Y. Zhang, M. S. Liu, Y. J. Cheng, A. K. Y. Jen, *Adv. Funct. Mater.* **2007**, *17*, 3808–3815; c) N, Kobayashi, R. Koguchi, M. Kijima, *Macromolecules* **2006**, *39*, 9102–9111; d) A. K. Mishra, M. Graf, F. Grasse, F. Jacob, E. J. W. List, K. Muellen, *Chem. Mater.* **2006**, *18*, 2879–2885.

[9] a) Y. Jin, J. Ju, J. Kim, S. Lee, J. Y. Kim, S. H. Park, S. M. Son, S. H. Jin, K. Lee, H. Suh, *Macromolecules* **2003**, *36*, 6970–6975; b) N. C. Greenham, S. C. Moratti, D. D. C. Bradley, R. H. Friend, A. B. Holmes, *Nature* **1993**, *365*, 628–630; c) S. C. Moratti, R. Cervini, A. B. Holmes, D. R. Baigent, R. H. Friend, N. C. Greenham, J. Grüner, P. J. Hamer, *Synth. Met.* **1995**, *71*, 2117–2120.

[10] a) J. L. Brédas, A. J. Heeger, *Chem. Phys. Lett.* **1994**, *217*, 507–512; b) M. S. Liu, X. Jiang, S. Liu, P. Herguth, A. K. Y. Jen, *Macromolecules* **2002**, *35*, 3532–3538; c) P. Herguth, Ph.D Thesis, University of Washington (USA), **2003**.

[11] a) M. S. Liu, X. Jiang, P. Herguth, A. K. Y. Jen, *Chem. Mater.* **2001**, *13*, 3820–3822; b) E. G. J. Staring, R. C. J. E. Demandt, D. Braun, G. L. J. Rikken, Y. A. R. R. Kessener, A. H. J. Venhuizen, M. M. F. van Knippenberg, M. Bouwmans, *Synth. Met.* **1995**, *71*, 2179–2180; c) A. Pucci, T. Biver, G. Ruggeri, I. L. Meza, Y. Pang, *Polymer* **2005**, *46*, 11198–11205; d) K. R. Yoon, H. Lee, *J. Mater. Sci.* **2005**, *40*, 5315–5317; e) G. S. Samal, A. K. Biswas, S. Singh, Y. N. Mohapatra, *Synth. Met.* **2005**, *155*, 303–305; f) F. Liang, Y. J. Pu, T. Kurata, J. Kido, H. Nishide, *Polymer* **2005**, *46*, 3767–3775; g) S. V. Chasteen, S. A. Carter, G. Rumbles, *J. Chem. Phys.* **2006**, *124*, 214704/1–214704/6; h) Y. Kuzuoka, Y. Yamaguchi, *Synth. Met.* **2008**, *158*, 489–496; i) G. Tu, H. Li, M. Forster, R. Heiderhoff, B. Ralf, J. Ludwig, U. Scherf, *Macromolecules* **2006**, *39*, 4327–4331.

[12] a) H. Y. Lin, G. S. Liou, W. Y. Lee, W. C. Chen, *J. Polym. Sci. Part A* **2007**, *45*, 1727–1736; b) C. Ego, A. C. Grimsdale, F. Uckert, G. Yu, G. Srdanov, K. Müllen, *Adv. Mater.* **2002**, *14*, 809–811; c) Q. Fang, T. Tamamoto, *Macromolecules* **2004**, *37*, 5894–5899; d) C. H. Chen, J. Shi, C. W. Tang, *Macromol. Symp.* **1997**, *125*, 1–48; e) J. H. Park, N. S. Cho, K. J. Young, H. J. Cho, H. K. Shim, H. Kim, Y. S. Lee, *Org. Electron.* **2007**, *8*, 272–285.

[13] P. Taranekar, M. Abdulbaki, R. Krishnamoorti, S. Phanichphant, P. Waenkaew, D. Patton, T. Fulghum, R. Advincula, *Macromolecules* **2006**, *39*, 3848–3854.

[14] L. Liao, Y. Pang, L. Ding, F. E. Karasz, *Macromolecules* **2004**, *37*, 3970–3972.

[15] J. Ding, M. Day, G. Robertson, J. Roovers, *Macromolecules* **2002**, *35*, 3474–3483.

[16] M. Fukuda, K. Sawada, K. Yoshino, *J. Polym. Sci. Part A* **1993**, *31*, 2465–2471.

[17] E. M. J. Johansson, P. G. Karlsson, M. Hedlund, D. Ryan, H. Siegbahn, H. Rensmo, *Chem. Mater.* **2007**, *19*, 2071–2978.

[18] J. A. Mikroyannidis, K. M. Gibbons, A. P. Kulkarni, S. A. Jenekhe, *Macromolcules* **2008**, *41*, 663–674.

[19] S. G. Smirnov, G. G. Konoplev, A. N. Rodionov, V. A. Godik, *J. Appl. Spectrosc.* **1983**, *38*, 658–664.

[20] Y. Lin, Y. Chen, M. Feng, A. X. Yan, X. D. Zhuang, *Nano. Res. Lett.* **2008**, *3*, 21–24.

[21] C. K. Mann, K. K. Barnes, *Electrochemical Reactions in Nonaqueous Systems*, Marcel Dekker, New York, **1990**.

[22] a) S. T. Brown, J. C. Rienstra-Kiracofe, H. F. Schaefer, *J. Phys. Chem. A* **1999**, *103*, 4065–4077; b) J. C. Rienstra-Kiracofe, C. J. Barden, S. T. Brown, H. F. Schaefer, *J. Phys. Chem. A* **2001**, *105*, 524–528.

[23] K. A. Nielsen, G. H. Sarova, L. Martin-Gomis, F. Fernandez-Lazaro, P. C. Stein, L. Sanguinet, E. Levillain, J. L. Sessler, D. M. Guldi, A. Sastre-Santos, J. O. Jeppesen, *J. Am. Chem. Soc.* **2008**, *130*, 460–462.

[24] a) C. Luo, M. Fujitsuka, A. Watanabe, O. Ito, L. Gan, Y. Huang, C.-H. Huang, *J. Chem. Soc. Faraday Trans.* **1998**, *94*, 527–532; b) K. Ohkubo, H. Kotani, J. Shao, Z. Ou, K. M. Kadish, G. Li, R. K. Pandey, M. Fujitsuka, O. Ito, H. Imahori, S. Fukuzumi, *Angew. Chem.* **2004**, *116*, 871–874; *Angew. Chem. Int. Ed.* **2004**, *43*, 853–856.

[25] The extinction coefficient of TPA$^{\cdot+}$ is estimated to be 2330 $M^{-1}cm^{-1}$ from recording the absorption spectra of a mixture of (CNF–TPA)$_n$ and [Ru(bpy)$_3$]$^{3+}$.

[26] Gaussian 03, Revision C.02, M. J. Frisch, G. W. Trucks, H. B. Schlegel, G. E. Scuseria, M. A. Robb, J. R. Cheeseman, J. A. Montgomery, Jr., T. Vreven, K. N. Kudin, J. C. Burant, J. M. Millam, S. S. Iyengar, J. Tomasi, V. Barone, B. Mennucci, M. Cossi, G. Scalmani, N. Rega, G. A. Petersson, H. Nakatsuji, M. Hada, M. Ehara, K. Toyota, R. Fukuda, J. Hasegawa, M. Ishida, T. Nakajima, Y. Honda, O. Kitao, H. Nakai, M. Klene, X. Li, J. E. Knox, H. P. Hratchian, J. B. Cross, V. Bakken, C. Adamo, J. Jaramillo, R. Gomperts, R. E. Stratmann, O. Yazyev, A. J. Austin, R. Cammi, C. Pomelli, J. W. Ochterski, P. Y. Ayala, K. Morokuma, G. A. Voth, P. Salvador, J. J. Dannenberg, V. G. Zakrzewski, S. Dapprich, A. D. Daniels, M. C. Strain, O. Farkas, D. K. Malick, A. D. Rabuck, K. Raghavachari, J. B. Foresman, J. V. Ortiz, Q. Cui, A. G. Baboul, S. Clifford, J. Cioslowski, B. B. Stefanov, G. Liu, A. Liashenko, P. Piskorz, I. Komaromi, R. L. Martin, D. J. Fox, T. Keith, M. A. Al-Laham, C. Y. Peng, A. Nanayakkara, M. Challacombe, P. M. W. Gill, B. Johnson, W. Chen, M. W. Wong, C. Gonzalez, J. A. Pople, Gaussian, Inc., Wallingford CT, 2004.